

Non-equilibrium Condensation Process in a Holographic Superconductor

Keiju Murata¹, Shunichiro Kinoshita² and Norihiro Tanahashi³

¹*DAMTP, University of Cambridge, Centre for Mathematical Sciences,
Wilberforce Road, Cambridge, CB3 0WA, United Kingdom*

^{2,3}*Yukawa Institute for Theoretical Physics, Kyoto University, Kyoto 606-8502, Japan*

October 14, 2018

Abstract

We study the non-equilibrium condensation process in a holographic superconductor. When the temperature T is smaller than a critical temperature T_c , there are two black hole solutions, the Reissner-Nordström-AdS black hole and a black hole with a scalar hair. In the boundary theory, they can be regarded as the supercooled normal phase and the superconducting phase, respectively. We consider perturbations on supercooled Reissner-Nordström-AdS black holes and study their non-linear time evolution to know about physical phenomena associated with rapidly-cooled superconductors. We find that, for $T < T_c$, the initial perturbations grow exponentially and, eventually, spacetimes approach the hairy black holes. We also clarify how the relaxation process from a far-from-equilibrium state proceeds in the boundary theory by observing the time dependence of the superconducting order parameter. Finally, we study the time evolution of event and apparent horizons and discuss their correspondence with the entropy of the boundary theory. Our result gives a first step toward the holographic understanding of the non-equilibrium process in superconductors.

¹K.Murata@damtp.cam.ac.uk

²kinosita@yukawa.kyoto-u.ac.jp

³tanahasi@yukawa.kyoto-u.ac.jp

1 Introduction

Over the past decade the AdS/CFT correspondence has received increasing attention and many studies have been made on it. It has been believed that the AdS/CFT correspondence plays a central role in the study of the strongly coupled region of quantum field theory because it is simply described by classical gravity theory on AdS spacetimes [1–3]. Recently, the duality between the superconductor and gravity theory has been proposed [4–6] as a new application of the AdS/CFT correspondence, in which the simplest gravity theory is given by Einstein-Maxwell-charged scalar theory with negative cosmological constant. In this gravity theory one of static solutions is the well-known Reissner-Nordström-AdS black hole solution, in which the scalar field vanishes. It is known that this solution is unstable when the temperature T is lower than a critical temperature T_c . In consequence of the instability, it is expected that the scalar field will condense into a non-vanishing profile and eventually the black hole will have the scalar hair breaking the $U(1)$ -gauge symmetry spontaneously. For low temperature $T < T_c$, such a static solution has been constructed numerically. It was shown that the solution has similar properties with superconductors [6]. Thus, the instability of the Reissner-Nordström-AdS black hole for low temperature was identified with the superconducting phase transition. In the same way, the Reissner-Nordström-AdS and hairy black holes in the gravitational theory were identified with the normal and superconducting phases of a superconductor realized within the dual field theory, respectively. Such holographic superconductors are considered as a hopeful approach to understand the property of strongly correlated electron systems.

The non-equilibrium process of strongly correlated systems such as superconductors is not fully understood because of difficulties in its theoretical treatment, and has been attracting much attention [7–11]. The AdS/CFT correspondence offers a novel approach to this longstanding problem. To understand non-equilibrium process of strongly correlated systems, we should simply solve classical dynamics of gravitational systems in the bulk thanks to the duality. Many attempts in this direction have been done to get insights for strongly coupled quark-gluon plasma, relativistic hydrodynamics and so on [12–21]. For near equilibrium dynamics of superconductor, there are several approaches from the holography. For example, transport coefficients, such as the electric conductivity, were obtained by the linear response theory [5, 6, 22]. (See also [23, 24] and references therein.) The static and dynamic critical phenomena were also studied in [25].¹ These studies played important rolls in understanding the holographic superconductor. However, very little progress has been made in the regime that the theory is far from equilibrium. In this paper, we give a holographic approach to understand the non-equilibrium process of superconductors.

As we mentioned before, for low temperature $T < T_c$ there are two phases of black holes in the gravity side, the Reissner-Nordström-AdS and the hairy black holes, and they are regarded as supercooled normal phase and superconducting phases, respectively. In this paper, we consider small perturbations on the supercooled Reissner-Nordström-AdS black holes and study non-linear time evolution of them. Because of the instability of the Reissner-Nordström-AdS black holes, the initial perturbations will grow exponentially at the beginning of the time evolution. It is expected that the exponential growth is saturated

¹ In addition, the superfluid hydrodynamics of this system has been discussed in [26, 27].

due to the non-linear effect and the spacetimes will approach static solutions. It is believed that the final states of the time evolution are the hairy black holes obtained in [6], but there is no proof.² Studying non-linear time evolutions of the Einstein-Maxwell-charged scalar system, we will show that the final states are given by the hairy black holes. We are also interested in dynamics of the phase transition on the boundary theory. To reveal the non-equilibrium process, we observe the time dependence of the superconducting order parameter and study how the normal phase goes to superconducting phase in the boundary theory in the middle of the time evolution. We also evaluate the relaxation time scale of the boundary theory. Finally, we study the time evolution of event and apparent horizons and discuss the correspondence with the entropy of the boundary theory.

The organization of this paper is as follows. In Section 2, we introduce the gravity theory of the holographic superconductor and give equations of motion. Assuming the plane symmetry, we obtain the (1+1)-dimensional partial differential equations (PDEs). We also give the outline of our calculations. In Section 3, we solve the equations of motion near the AdS boundary in order to obtain boundary conditions at the AdS boundary. In Section 4, we explain the numerical method to solve the equations of motion. In Section 5, we give the numerical results of non-linear time evolution. We find that the final states of the time evolutions coincide with the hairy black holes for general initial conditions. In the middle of time evolution, we study the time dependence of superconducting order parameters and measure the relaxation time of them. The time evolutions of event and apparent horizons are also studied. The final section is devoted to conclusions.

2 Equations of motion

We consider the 4-dimensional Einstein-Maxwell-charged scalar theory with negative cosmological constant, whose action is given by

$$S = \int d^4x \sqrt{-g} \left[R + \frac{6}{L^2} - \frac{1}{4} F_{\mu\nu} F^{\mu\nu} - |\partial_\mu \psi - iq A_\mu \psi|^2 - m^2 |\psi|^2 \right], \quad (2.1)$$

where L is the AdS curvature scale and q is the $U(1)$ -charge of the complex scalar field ψ . The field strength is defined by $F = dA$ as usual. This theory is introduced in [4–6] as a gravity dual of a superconductor. In addition to the diffeomorphism symmetry, this action has the local $U(1)$ symmetry,

$$A \rightarrow A + d\lambda, \quad \psi \rightarrow e^{iq\lambda} \psi, \quad (2.2)$$

where λ is an arbitrary scalar function. Hereafter, we take the unit of $L = 1$.

For simplicity, we assume that the spacetime has the plane symmetry. Using the diffeomorphism and $U(1)$ gauge symmetries together with the assumed plane symmetry, we can take the metric ansatz without loss of generality as

$$\begin{aligned} ds^2 &= -\frac{1}{z^2} [F(t, z) dt^2 + 2dt dz] + \Phi(t, z)^2 (dx^2 + dy^2), \\ A &= \alpha(t, z) dt, \\ \psi &= \psi(t, z). \end{aligned} \quad (2.3)$$

²Recently, evidence of this conjecture has been given in [28] in the near critical temperature regime.

We use the ingoing Eddington-Finkelstein coordinates, (t, z) . In these coordinates, the AdS boundary is located at $z = 0$. These coordinates are convenient for our numerical calculations since we can easily extend time slices defined by constant- t surfaces into the inside of the event horizon and also set the AdS boundary to be a constant- z plane. Note that diffeomorphism and $U(1)$ gauge symmetries have not been completely fixed, because the form of the variables (2.3) is invariant under the residual symmetry, $1/z \rightarrow 1/z + g(t)$, $\alpha \rightarrow \alpha + \partial_t \lambda(t)$ and $\psi \rightarrow e^{iq\lambda(t)}\psi$. These residual gauge symmetries will be fixed by the boundary conditions. The complete set of the equations of motion are given by

$$(\Phi D\Phi)' - \frac{\Phi^2}{4z^2} \left(\frac{1}{2}z^4\alpha'^2 + m^2|\psi|^2 - 6 \right) = 0, \quad (2.4)$$

$$2z^2(D\psi)' + iqz^2\alpha'\psi + 2z^2\Phi^{-1}(D\Phi)\psi' + 2z^2\Phi^{-1}\Phi'D\psi + m^2\psi = 0, \quad (2.5)$$

$$(z^2(z^{-2}F)')' - z^2\alpha'^2 + 4\Phi^{-2}(D\Phi)\Phi' - (\psi^{*'}D\psi + \psi'D\psi^*) = 0, \quad (2.6)$$

$$2z^2(D\alpha)' + z^4(z^{-2}F)'\alpha' + 4z^2\Phi^{-1}(D\Phi)\alpha' - 2iq(\psi D\psi^* - \psi^* D\psi) = 0, \quad (2.7)$$

and

$$\Phi^{-2}C_1 \equiv -2\Phi^{-1}D^2\Phi - \left(F' - \frac{2}{z}F \right) \Phi^{-1}D\Phi - |D\psi|^2 = 0, \quad (2.8)$$

$$\Phi^{-2}C_2 \equiv -2z^3\Phi^{-1}(z\Phi'' + 2\Phi') - z^4|\psi'|^2 = 0, \quad (2.9)$$

$$\Phi^{-2}C_3 \equiv -z^2[z^2\alpha'' + 2z\alpha' + 2z^2\Phi^{-1}\Phi'\alpha' + iq(\psi\psi^{*'} - \psi^*\psi')] = 0, \quad (2.10)$$

where $' \equiv \partial_z$ and derivative operator D is defined as

$$\begin{aligned} D\Phi &= \partial_t\Phi - F\partial_z\Phi/2, & D^2\Phi &= \partial_t(D\Phi) - F\partial_z(D\Phi)/2, & D\alpha &= \partial_t\alpha - F\partial_z\alpha/2, \\ D\psi &= \partial_t\psi - F\partial_z\psi/2 - iq\alpha\psi, & D\psi^* &= \partial_t\psi^* - F\partial_z\psi^*/2 + iq\alpha\psi^*. \end{aligned} \quad (2.11)$$

Here, the operator $\partial_t - F\partial_z/2$ represents the derivative along the outgoing null vector. We regard Eqs. (2.4-2.7) as evolution equations and Eqs. (2.8-2.10) as constraint equations. The constraint equations satisfy

$$\partial_z C_1 = 0, \quad (2.12)$$

$$DC_2 = z^2\partial_z(F/z^2)C_2 + \frac{1}{2}z^2(\partial_z\alpha)C_3, \quad (2.13)$$

$$DC_3 = \frac{1}{2}z^2\partial_z(F/z^2)C_3, \quad (2.14)$$

where $DC_i = \partial_t C_i - F\partial_z C_i/2$ ($i = 2, 3$). To derive the above equations, we have used evolution equations (2.4-2.7). As we can see from Eqs. (2.12-2.14), the evolution equations guarantee that the constraint equations to be satisfied if $C_1 = 0$ and $C_2 = C_3 = 0$ are satisfied on the AdS boundary ($z = 0$) and on the initial surface ($t = 0$), respectively. Therefore, we solve the evolution equations for the time evolution and use the constraint equations only at the AdS boundary and the initial surface to give the boundary conditions for the time evolution.

One of static solutions of the equations of motion is merely the Reissner-Nordström-AdS black hole solution (with planar horizon), which is given by

$$F = 1 - 2Mz^3 + \frac{1}{4}Q^2z^4, \quad \Phi = \frac{1}{z}, \quad \alpha = Qz, \quad \psi = 0. \quad (2.15)$$

Parameters M and Q are proportional to mass and charge of the black hole, respectively. For this solution, the complex scalar field has a trivial configuration $\psi = 0$. That is, this black hole has no “hair” except for the mass and electric charge. The event horizon is located at $z = z_+$ determined by $F(z_+) = 0$. In terms of the horizon radius z_+ , we can rewrite M as

$$M = \frac{1}{2z_+^3} \left(1 + \frac{1}{4} Q^2 z_+^4 \right) . \quad (2.16)$$

The temperature of the black hole is given by

$$T = - \frac{1}{4\pi} \frac{dF}{dz} \Big|_{z=z_+} = \frac{12 - z_+^4 Q^2}{16\pi z_+} . \quad (2.17)$$

It is known that this solution is unstable when the temperature T is smaller than a critical temperature T_c . The numerical value of the T_c is obtained in [4–6]. In consequence of the instability, it is expected that the scalar field will grow and eventually the black hole will have the scalar hair. Thus, the $U(1)$ -gauge symmetry is spontaneously broken due to condensation of the complex scalar field. Indeed, for low temperature $T < T_c$ at fixed charge Q , static solutions of the hairy black hole with $\psi \neq 0$ exist and have been constructed numerically [6]. Similarly to the previous case, the temperature of the hairy black hole is given by

$$T = - \frac{1}{4\pi} \frac{dF}{dz} \Big|_{z=z_+} , \quad (2.18)$$

where $F(z_+) = 0$.

This instability was identified with the superconducting phase transition in the dual theory [4–6]. In this paper, we will investigate the dynamical process of the superconducting phase transition in the view of the gravity theory. We show the schematic of our setting in Figure 1. Since we are taking the ingoing Eddington-Finkelstein coordinates (2.3), our time slices are given by null surfaces. We consider a slightly-perturbed Reissner-Nordström-AdS spacetime as initial data, and study non-linear time evolution from it. At the AdS boundary, we give appropriate boundary conditions, as we explain in the subsequent section. Inside the event horizon, we excise a region before encountering the singularity for the numerical calculation. The detailed procedure will be explained in following sections.

3 Asymptotic expansion

Now, we determine the asymptotic form of the variables at the AdS boundary $z = 0$ to clarify the boundary conditions for the time evolution. Hereafter, we set the mass of the complex scalar field as $m^2 = -2L^{-2}$ following [5, 6]. Then, we can expand variables as

$$\begin{aligned} F(t, z) &= 1 + F_1(t)z + F_2(t)z^2 + F_3(t)z^3 + \cdots , \\ \Phi(t, z) &= 1/z + \Phi_0(t) + \Phi_1(t)z + \Phi_2(t)z^2 + \Phi_3(t)z^3 + \cdots , \\ \alpha(t, r) &= \alpha_0(t) + \alpha_1(t)z + \alpha_2(t)z^2 + \alpha_3(t)z^3 + \cdots , \\ \psi(t, r) &= \psi_1(t)z + \psi_2(t)z^2 + \psi_3(t)z^3 + \cdots . \end{aligned} \quad (3.1)$$

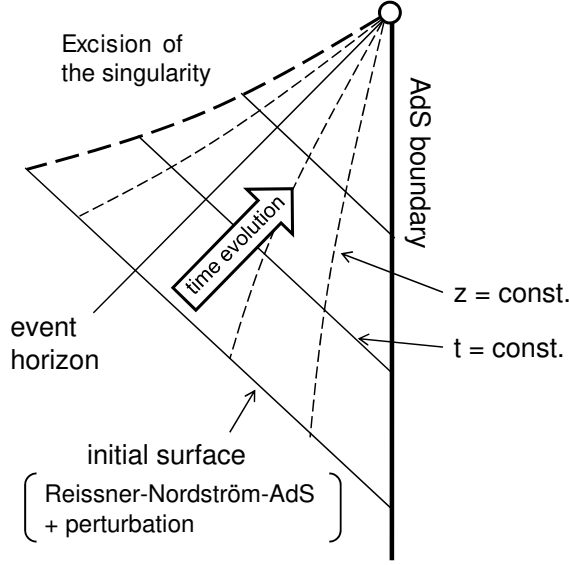


Figure 1: Schematic of our setting. We take the ingoing Eddington-Finkelstein coordinates, in which time slices are given by null surfaces. We consider a small perturbation on the Reissner-Nordström-AdS spacetime as initial data on an initial surface and study its non-linear time evolution.

Using residual gauge symmetries $1/z \rightarrow 1/z + g(t)$ and $\alpha \rightarrow \alpha + \partial_t \lambda(t)$, we put $\Phi_0(t) = 0$ and $\alpha_0(t) = 0$. Substituting Eq. (3.1) into Eqs. (2.4-2.10) and solving the equations order by order, we obtain the expansion coefficients as

$$\begin{aligned}
F_1 &= 0, & F_2 &= -\frac{1}{2}\psi_1\psi_1^*, & \dot{F}_3 &= \frac{1}{2}[\psi_1^*\ddot{\psi}_1 + \psi_1\ddot{\psi}_1^* - \psi_1\dot{\psi}_2^* - \psi_1^*\dot{\psi}_2] \\
\Phi_1 &= -\frac{1}{4}|\psi_1|^2, & \Phi_2 &= -\frac{1}{6}(\psi_1\psi_2^* + \psi_1^*\psi_2), \\
\Phi_3 &= -\frac{1}{6}|\psi_2|^2 - \frac{11}{96}|\psi_1|^4 - \frac{1}{8}(\psi_1\dot{\psi}_2^* + \psi_1^*\dot{\psi}_2) \\
\dot{\alpha}_1 &= -iq(-\psi_2\psi_1^* + \psi_1\psi_2^* + \dot{\psi}_1\psi_1^* - \psi_1\dot{\psi}_1^*), & \alpha_2 &= -\frac{1}{2}iq(-\psi_2\psi_1^* + \psi_1\psi_2^*), \\
\psi_3 &= -\frac{1}{2}iq\alpha_1\psi_1 + \dot{\psi}_2 + \frac{1}{2}\psi_1^2\psi_1^*,
\end{aligned} \tag{3.2}$$

where $\dot{} \equiv d/dt$. We find that all the coefficients $F_i(t)$, $\Phi_i(t)$, $\alpha_i(t)$ and $\psi_i(t)$ can be expressed by $\psi_1(t)$ and $\psi_2(t)$. This means that if the two functions $\psi_1(t)$ and $\psi_2(t)$ are given at the boundary we can determine the bulk in principle. It is noticed that these are order parameters characterizing normal and superconducting phases in the boundary theory [5,6]. In our calculation, we do not give $\psi_2(t)$ at $z = 0$, and $\psi_2(t)$ is determined as a result of the time evolution. As for the inner boundary, a constant- z surface, no boundary condition is required there since it will be a spacelike surface as long as we take it behind the horizon.

Note that initial values of $F_3(t)$ and $\alpha_1(t)$ are not determined by the asymptotic expansion, because the asymptotic expansion gives just time derivative of $F_3(t)$ and $\alpha_1(t)$. In fact, $F_3(t)$ and $\alpha_1(t)$ are related to with mass and charge of the system. Hence initial values of $F_3(t)$ and $\alpha_1(t)$ represent the initial mass and charge of black holes. We put the

initial mass and charge as M_0 and Q_0 , respectively and, then, F_3 and α_1 are written as

$$\begin{aligned}
F_3 &\equiv -2M(t) \\
&= -2M_0 + \frac{1}{2} \int_0^t dt [\psi_1^* \ddot{\psi}_1 + \psi_1 \ddot{\psi}_1^* + \dot{\psi}_1 \dot{\psi}_2^* + \dot{\psi}_1^* \dot{\psi}_2] - \frac{1}{2} \left[\psi_1 \psi_2^* + \psi_1^* \psi_2 \right]_0^t, \\
\alpha_1 &\equiv Q(t) \\
&= Q_0 - iq \int_0^t dt [-\psi_2 \psi_1^* + \psi_1 \psi_2^* + \dot{\psi}_1 \dot{\psi}_1^* - \psi_1 \dot{\psi}_1^*],
\end{aligned} \tag{3.3}$$

where $M(t)$ and $Q(t)$ denote the total mass and charge, respectively.

4 A method to solve equations of motion

In this section, we explain a method to solve the equations of motion numerically³. From Eq. (3.2), we can see that the first few expansion coefficients in Eq. (3.1) do not depend on $\psi_2(t)$ but only on $\psi_1(t)$. In our calculation, we give $\psi_1(t)$ as a boundary condition at $z = 0$. Moreover, some variables have divergent parts whose form is fully determined by the asymptotically-AdS boundary conditions. Thus, it is reasonable for numerical calculations to define new regular variables $\tilde{\Phi}$, $\tilde{\psi}$ and \tilde{F} as

$$\begin{aligned}
\Phi &= 1/z + z\Phi_1(t) + z^2\tilde{\Phi}(t, z), \\
\psi &= z\psi_1(t) + z^2\tilde{\psi}(t, z), \\
F &= 1 + zF_1(t) + z^2F_2(t) + z^3\tilde{F}(t, z),
\end{aligned} \tag{4.1}$$

where $\Phi_1(t)$, $F_1(t)$ and $F_2(t)$ are given by Eq. (3.2) and they do not depend on $\psi_2(t)$ but only on $\psi_1(t)$. Note that by these definitions we have $\psi_2(t) = \tilde{\psi}(t, z)|_{z=0}$. We also define $\tilde{D}\Phi$ and $\tilde{D}\psi$ as

$$\begin{aligned}
\tilde{D}\Phi &= 1/(2z^2) + \Phi_1(t)/2 + F_2(t)/2 + z\tilde{D}\Phi(t, z), \\
\tilde{D}\psi &= -\psi_1(t)/2 + z\tilde{D}\psi(t, z).
\end{aligned} \tag{4.2}$$

From Eq. (2.11), $\tilde{D}\Phi$ and $\tilde{D}\psi$ can be written in terms of $\tilde{\Phi}$ and $\tilde{\psi}$ as

$$\begin{aligned}
2\tilde{D}\Phi &= 2\dot{\Phi}_1 - 2\tilde{\Phi} + \tilde{F} + z(2\partial_t\tilde{\Phi} - \partial_z\tilde{\Phi} - F_2\Phi_1) \\
&\quad - z^2(2F_2\tilde{\Phi} + \Phi_1\tilde{F}) - z^3(F_2\partial_z\tilde{\Phi} + 2\tilde{F}\tilde{\Phi}) - z^4\tilde{F}\partial_z\tilde{\Phi},
\end{aligned} \tag{4.3}$$

$$\begin{aligned}
2\tilde{D}\psi &= 2\dot{\psi}_1 - 2\tilde{\psi} + z(2\partial_t\tilde{\psi} - \partial_z\tilde{\psi} - F_2\psi_1) \\
&\quad - z^2(2F_2\tilde{\psi} + \psi_1\tilde{F}) - z^3(F_2\partial_z\tilde{\psi} + 2\tilde{\psi}\tilde{F}) - z^4\tilde{F}\partial_z\tilde{\psi}.
\end{aligned} \tag{4.4}$$

In terms of $\tilde{\Phi}$, $\tilde{\psi}$, \tilde{F} , $\tilde{\Phi}$, $\tilde{\psi}$, $\tilde{D}\Phi$ and $\tilde{D}\psi$, we can rewrite evolution equations (2.4-2.7) as

$$(\tilde{D}\Phi)' + X_1[\tilde{\Phi}]\tilde{D}\Phi + X_2[\tilde{\Phi}, \tilde{\psi}, \alpha] = 0, \tag{4.5}$$

$$(\tilde{D}\psi)' + Y[\tilde{D}\Phi, \tilde{\Phi}, \tilde{\psi}, \alpha] = 0, \tag{4.6}$$

$$(z^2\tilde{F})'' + Z[\tilde{D}\Phi, \tilde{D}\psi, \tilde{\Phi}, \tilde{\psi}, \alpha] = 0, \tag{4.7}$$

$$(D\alpha)' + W[\tilde{D}\Phi, \tilde{D}\psi, \tilde{\Phi}, \tilde{\psi}, \alpha, \tilde{F}] = 0, \tag{4.8}$$

³Similar calculations were performed in [21] in the context of the AdS/QGP.

and constraint equations (2.9) and (2.10) as ⁴

$$\tilde{\Phi}'' + P_1[\tilde{\Phi}]\tilde{\Phi}' + P_2[\tilde{\Phi}, \tilde{\psi}] = 0 , \quad (4.9)$$

$$\alpha'' + Q_1[\tilde{\Phi}]\alpha' + Q_2[\tilde{\psi}] = 0 . \quad (4.10)$$

where $X_1, X_2, Y, Z, W, P_1, P_2, Q_1$ and Q_2 are functions of each arguments. Since the expression of these functions are tedious, we do not write their explicit expressions.

The procedure to solve Eqs. (4.5-4.10) as follows. To begin with, we must construct initial data of $\tilde{\Phi}(t = 0, z)$, $\tilde{\psi}(t = 0, z)$ and $\alpha(t = 0, z)$ on the initial surface $t = 0$ that satisfy the constraint equations (4.9) and (4.10).

1. On the initial surface $t = 0$, we prepare initial data of $\tilde{\psi}(t = 0, z)$, initial mass M_0 and charge Q_0 .
2. Integrating Eq. (4.9) and (4.10) from $z = 0$ to $z = z_0$, we can obtain initial data $\tilde{\Phi}(t = 0, z)$ and $\alpha(t = 0, z)$. Here, $z = z_0$ is the boundary of computational domain, which we set to be between the horizon and the black hole singularity. For these radial integrations, we need boundary conditions $\tilde{\Phi}(t = 0, z)|_{z=0}$ and $\alpha(t = 0, z)|_{z=0}$. They are given by the asymptotic expansion (3.1) as

$$\begin{aligned} \tilde{\Phi}(t = 0, z)|_{z=0} &= \Phi_2(0) , & \partial_z \tilde{\Phi}(t = 0, z)|_{z=0} &= \Phi_3(0) , \\ \alpha(t = 0, z)|_{z=0} &= 0 , & \partial_z \alpha(t = 0, z)|_{z=0} &= \alpha_1(0) , \end{aligned} \quad (4.11)$$

where coefficients $\Phi_2(0)$, $\Phi_3(0)$ and $\alpha_1(0)$ are written by $\psi_1(0)$ and $\psi_2(0)$ as shown in Eq. (3.2). The $\psi_2(0)$ can be read off from $\tilde{\psi}(t = 0, z)|_{z=0}$.

Once we have obtained the data of $\tilde{\Phi}(t, z)$, $\tilde{\psi}(t, z)$ and $\alpha(t, z)$ on a constant- t surface at an arbitrary time t , we can calculate the data of $\tilde{\Phi}(t + \delta t, z)$, $\tilde{\psi}(t + \delta t, z)$ and $\alpha(t + \delta t, z)$ on the next time slice $t + \delta t$ as follows.

- i. Integrating Eqs. (4.5-4.8) from $z = 0$ to $z = z_0$, we obtain the $\tilde{D}\tilde{\Phi}$, $\tilde{D}\tilde{\psi}$, $D\alpha$ and \tilde{F} on the constant- t surface, on which $\tilde{\Phi}(t, z)$, $\tilde{\psi}(t, z)$ and $\alpha(t, z)$ have been known. Boundary conditions for the radial integration are given by the asymptotic expansion (3.1) as

$$\begin{aligned} \tilde{D}\tilde{\Phi}(t, z)|_{z=0} &= -\Phi_2(t) + \frac{1}{2}F_3(t) - \frac{1}{4}(\psi_1(t)\dot{\psi}_1^*(t) + \psi_1^*(t)\dot{\psi}_1(t)) , \\ \tilde{D}\tilde{\psi}(t, z)|_{z=0} &= \dot{\psi}_1(t) - \psi_2(t) , & D\alpha(t, z)|_{z=0} &= -\frac{1}{2}\alpha_1(t) \\ z^2\tilde{F}(t, z)|_{z=0} &= 0 , & \partial_z[z^2\tilde{F}(t, z)]|_{z=0} &= 0 . \end{aligned} \quad (4.12)$$

where $\Phi_2(t)$, $F_3(t)$ and $\alpha_1(t)$ are written by $\psi_1(t)$ and $\psi_2(t)$ as in Eq. (3.2) and (3.3).

- ii. We calculate $\partial_t\tilde{\Phi}(t, z)$, $\partial_t\alpha(t, z)$ and $\partial_t\tilde{\psi}(t, z)$ from Eq. (2.11). We use the upwind differencing scheme for advection terms in Eq. (2.11).

⁴ We do not use Eq. (2.8), one of the constraint equations, hereafter. This equation has been already used to derive the asymptotic form of the variables (3.2). In our calculations, Eq. (2.8) will be guaranteed to be satisfied by the boundary conditions (3.2).

- iii. We obtain variables $\tilde{\Phi}(t + \delta t, z)$, $\tilde{\psi}(t + \delta t, z)$ and $\alpha(t + \delta t, z)$ on the next time slice $t + \delta t$ by using time derivative of each variables $\partial_t \Phi(t, z)$, $\partial_t \alpha(t, z)$ and $\partial_t \psi(t, z)$.

By repeating the above procedure i \sim iii, we can numerically calculate time evolution of the system.

5 Non-equilibrium Condensation Process

In this section, we summarize the numerical results obtained by the evolution scheme of the previous section. In Section 5.1, we describe the free parameter and the initial conditions. We summarize the general properties of the bulk field dynamics in Section 5.2. After that, we study the dynamics of the order parameter of the boundary theory, which is the boundary value of the bulk scalar field, in Section 5.3. We also investigate its growth and decay rates around the initial and final states in Section 5.4. In Section 5.5, we focus on the dynamics of the event and the apparent horizons. If a black hole is stationary, then the entropy of the boundary theory, which is another important physical quantity, will be straightforwardly identified with the horizon area in the bulk. However, it is not so obvious in dynamical cases. In order to argue their relevance to the boundary theory entropy, we clarify to what extent the bulk spacetime is dynamical and give some consideration on how to identify the boundary and the bulk spacetime in Section 5.6.

5.1 Initial data and parameters

As explained in Section 4, we should specify the $\tilde{\psi}(t = 0, z)$, M and Q on the initial surface. We treat M and Q as fixed parameters in this section since they are conserved quantities in our setting as we will see later. Without loss of generality, we can fix one of the parameters using the scaling symmetry⁵,

$$(t, z, x, y) \rightarrow (kt, kz, kx, ky) , \quad (5.1)$$

$$F \rightarrow F , \quad \Phi \rightarrow \Phi/k , \quad \alpha \rightarrow \alpha/k , \quad \psi \rightarrow \psi , \quad (5.2)$$

$$M \rightarrow M/k^3 , \quad Q \rightarrow Q/k^2 , \quad T \rightarrow T/k . \quad (5.3)$$

Using this scaling symmetry, in our numerical calculation, we put

$$M = \frac{1}{2} \left(1 + \frac{1}{4} Q^2 \right) . \quad (5.4)$$

This condition implies that the *horizon radius* of the initial black hole is set to unity (see Eq. (2.16))⁶. As for the initial data of $\tilde{\psi}$, we consider the Gaussian perturbation on the Reissner-Nordström-AdS spacetime as

$$\tilde{\psi}(t = 0, z) = \frac{\mathcal{A}}{\sqrt{2\pi} \delta} \exp \left[-\frac{(z - z_m)^2}{2\delta^2} \right] \quad (5.5)$$

⁵This is just a residual coordinate transformation which preserves the form of metric and gauge field in Eq. (2.3) as well as the boundary conditions $F(t, z) \simeq 1$ and $\Phi(t, z) \simeq 1/z$ for $z \rightarrow 0$.

⁶To be accurate, the z_+ defined by Eq. (2.16) slightly differs from the apparent horizon position for our initial data, because we will give small perturbations on the Reissner-Nordström-AdS solutions.

with $\mathcal{A} = 0.01$, $\delta = 0.05$ and $z_m = 0.3$. We tried several other initial conditions and found that they yield qualitatively the same results. Thus, we will show below the results only for the initial data given by Eq. (5.5).

5.2 Dynamics of bulk fields

First of all, we show the dynamics of the bulk scalar field. As we mentioned before, our numerical calculation is performed under the boundary condition $\psi_1(t) = 0$ at the AdS boundary $z = 0$. This means that we regard $\psi_2(t)$ as the order parameter of condensation. Furthermore, it turns out from Eq. (3.3) that F_3 and α_1 become time-independent when $\psi_1(t) = 0$, namely the total mass M and the total charge Q are conserved in our calculation.

In Figure 2, we depict the dynamics of the amplitude of the complex scalar, $|\psi(t, z)|$, for $q = 1.0$ and $T/T_c = 0.5$ at the initial state. The critical temperature T_c is evaluated for a fixed charge Q^7 . We can find that much of the wave packet of the initial perturbation (5.5) is instantaneously absorbed in the horizon within $tT_c \lesssim 0.06$. Because of the remnant of the wave packet, which is the unstable mode contained in the initial perturbation (5.5), the scalar density grows exponentially for $tT_c \lesssim 6$. The exponential growth is saturated by the nonlinear effect at $tT_c \sim 6$. In $tT_c \gtrsim 6$, the scalar density approaches a static solution. As in Figure 3, we can find that the static solution coincides with the hairy black hole solution obtained in [6]. Thus, our result gives numerical proof of the conjecture that the final state of the instability of the Reissner-Nordström-AdS black hole is the hairy black hole. Our result also implies that, for the plane-symmetric perturbations, the hairy black holes are stable. It is worth noting that this phase transition from the initial Reissner-Nordström-AdS black hole to the final hairy black hole is a dynamical process under the fixed mass and charge. It implies that the temperature of the initial state and that of the final state are different in general. Indeed, the temperature of the final hairy black hole increases compared to the initial temperature due to the phase transition.

5.3 Dynamics of the order parameter

In following subsections, we show some results from the numerical solutions that are relevant to the dual theory. In this subsection, we describe the non-linear dynamics of the order parameter of the boundary theory.

From the asymptotic form of the numerical solution $\psi(t, z)$, we can read off $\psi_2(t)$ defined by Eq. (3.1). The coefficient $\psi_2(t)$ is regarded as the superconducting order parameter in dual theory. Following [5, 6], we define the order parameter on the boundary theory as

$$\langle \mathcal{O}_2(t) \rangle \equiv \sqrt{2} \psi_2(t) . \quad (5.6)$$

In Figure 4, we depict the time dependence of the order parameter $(q|\langle \mathcal{O}_2(t) \rangle|)^{1/2}/T_c$, which is invariant under the scaling (5.3), for $q = 1.5$ and $T/T_c = 0.2, 0.4, 0.6, 0.8, 1.1, 1.2$ and

⁷In this section, we investigate the time evolution of the scale invariant variables under the scaling symmetry (5.3). For $q = 1.0, 1.5$ and 2.0 , the critical temperature T_c is respectively given by $T_c/\sqrt{Q} = 0.03589, 0.08421$ and 0.1234 .

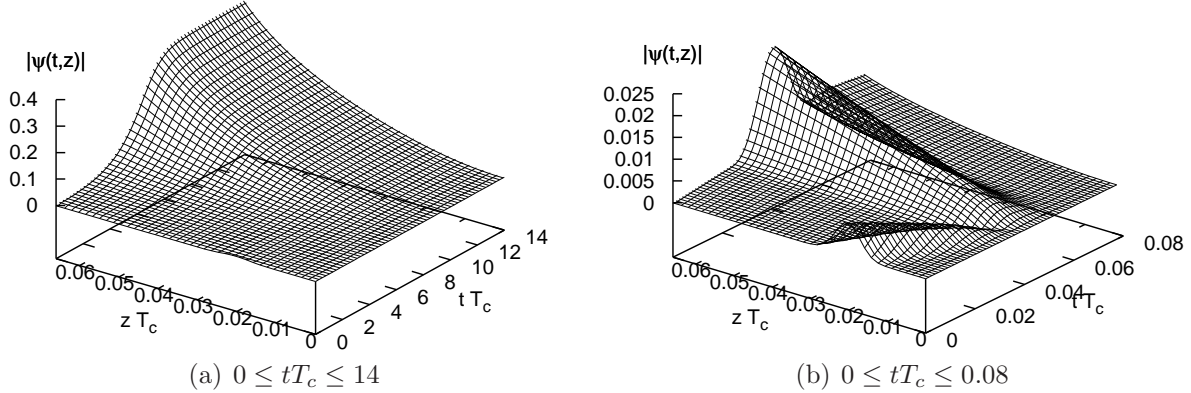


Figure 2: The dynamics of the scalar field for $q = 1.0$ and initial temperature $T/T_c = 0.5$. In Figure (a), we depict the dynamics of the amplitude of the complex scalar field, $|\psi(t, z)|$, on (t, z) -plane for $0 \leq tT_c \leq 14$. Because of the instability of the Reissner-Nordström-AdS black hole, the scalar density grows exponentially for $tT_c \lesssim 6$. We find that, for $tT_c \gtrsim 6$, the scalar density approaches some static function. In Figure (b), we depict $|\psi(t, z)|$ for $0 \leq tT_c \leq 0.08$ in order to focus on the behavior of the wave packet of the initial perturbation. We can see that the wave packet is reflected by the AdS boundary at $t \simeq 0.04$ and much of the wave packet is absorbed in the black hole horizon within $tT_c \lesssim 0.06$.

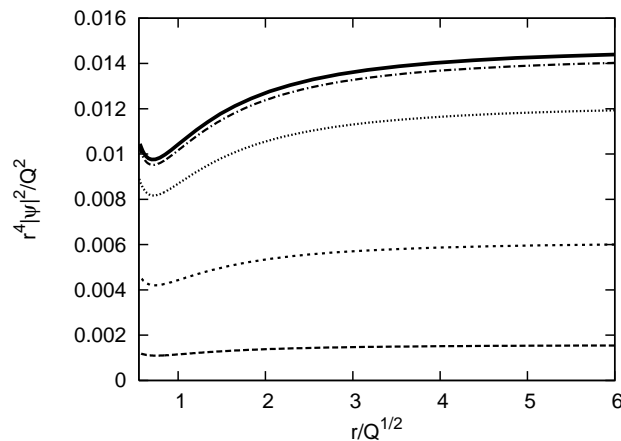


Figure 3: The function $r^4|\psi|^2/Q^2$ is depicted on fixed time slices, where r is circumference radius defined by $r = \Phi$. From bottom to top, the curves correspond to $tT_c = 5.15, 6.44, 7.73$ and 9.02 . The top solid curve correspond to that of the hairy black hole. We can see that the solution approaches the hairy black hole.

1.4. The sharp signal at the small t is caused by the initial perturbation (5.5). For $T > T_c$, the initial perturbation dissipates and the order parameter converges to zero. On the other hand, for $T < T_c$, the order parameter grows exponentially and approaches a non-trivial value. We find that, for $T < T_c$, the more rapidly the order parameter converges to its final value for lower temperature.

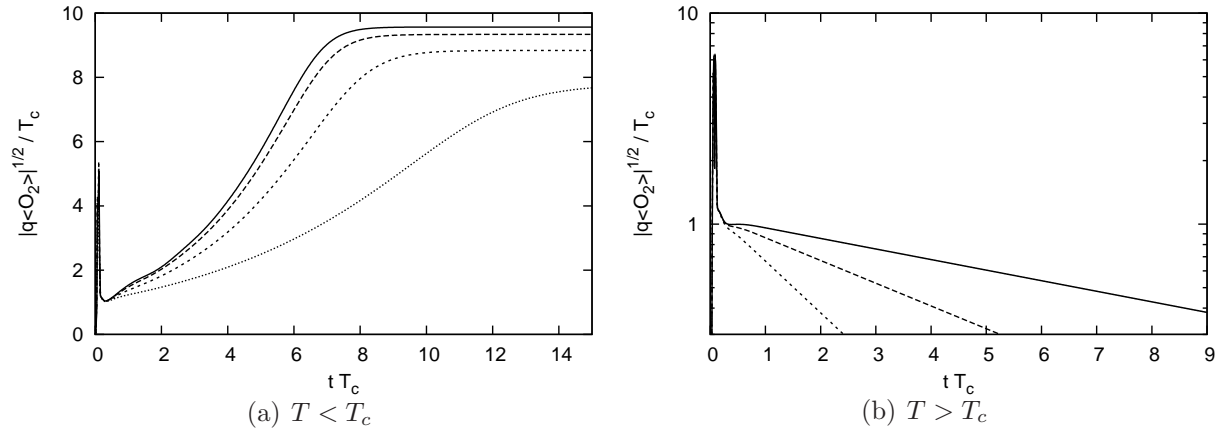


Figure 4: The dynamics of the order parameter is depicted for $q = 1.5$. In Figure (a), the curves from top to bottom correspond to $T/T_c = 0.2, 0.4, 0.6$ and 0.8 . In Figure (b), the curves from top to bottom correspond to $T/T_c = 1.1, 1.2$ and 1.4 . Note that the vertical axis in Figure (b) is logarithmic scale, while that is linear scale in Figure (a).

5.4 Growth and decay rates

In this subsection, we estimate the growth and decay rates of the order parameter. At the beginning of the time evolution, namely, around the normal phase $\langle \mathcal{O}_2(t) \rangle = 0$, we fit the time dependence of the order parameter as

$$|\langle \mathcal{O}_2(t) \rangle| = C \exp(-t/t_{\text{relax}}) , \quad (5.7)$$

where C and t_{relax} are constants and t_{relax} represents the relaxation time scale. In Figure 5(a), we depict the $1/t_{\text{relax}}$ around the normal phase against the temperature for $q = 1.0, 1.5$ and 2.0 . For $T < T_c$, $1/t_{\text{relax}}$ has negative value since the initial Reissner-Nordström-AdS black holes are unstable. At the onset of the instability $T = T_c$, the $1/t_{\text{relax}}$ becomes zero. It seems that, for $T/T_c \rightarrow 0$, $1/t_{\text{relax}}$ does not diverge, but converges to finite value.

For $T < T_c$, the order parameter condenses into the non-trivial value. Around the condensed phase, we fit the time dependence of the order parameter as

$$|\langle \mathcal{O}_2(t) \rangle| = C_1 \exp(-t/t_{\text{relax}}) + C_2 , \quad (5.8)$$

where C_1 and C_2 are constants. In Figure 5(b), we depict the $1/t_{\text{relax}}$ around the condensed phase against the temperature. Note that we used in this figure the temperature of the final state of the time evolution, that is, the hairy black hole. We find that, at $T \rightarrow T_c$, $1/t_{\text{relax}}$ approaches zero. On the other hand, for $T/T_c \rightarrow 0$, $1/t_{\text{relax}}$ has larger value as the temperature becomes lower.

In the gravity side, the $1/t_{\text{relax}}$ is nothing but the imaginary part of the quasinormal frequency of the fundamental mode. For the normal phase, which is the Reissner-Nordström-AdS black hole, quasinormal modes are studied in [22, 29, 30]. For the condensed phase, which is the hairy black hole, quasinormal modes are studied in the decoupling limit $q \rightarrow \infty$ in [22]. The result in Figure 5(b) gives the quasinormal frequency of the hairy black holes with the back-reaction on the gravitational field.

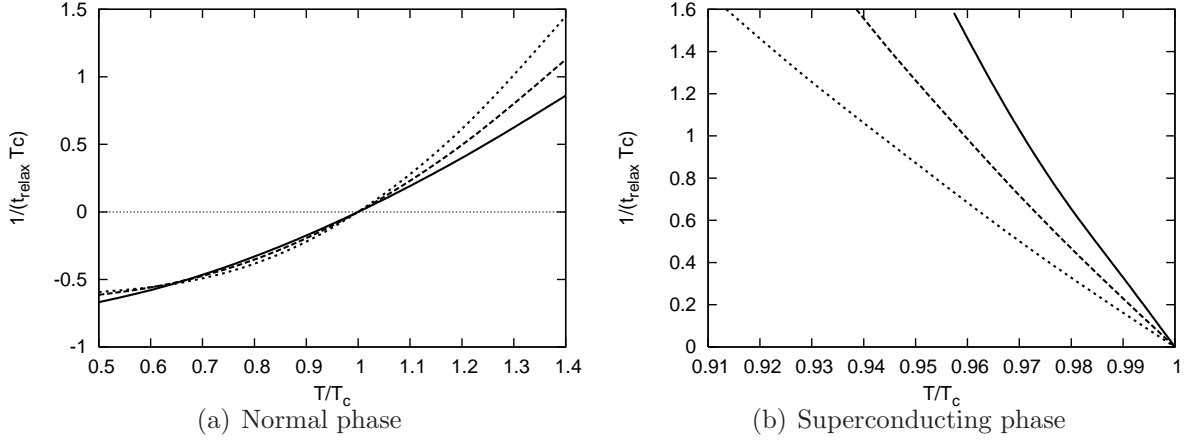


Figure 5: The relaxation times t_{relax} of the order parameter against the temperature T . Figure (a) and (b) shows the relaxation time around the normal and the condensed phases, respectively. The solid, dashed and dotted curves correspond to $q = 1.0, 1.5$ and 2.0 . In Figure (b), we used the temperature of the final state of the time evolution, that is, the hairy black hole.

5.5 Evolution of horizons

Now, we investigate the time evolution of apparent and event horizons. The apparent horizon $z = z_{\text{AH}}(t)$ can be determined from

$$D\Phi(t, z_{\text{AH}}(t)) = 0 . \quad (5.9)$$

We determine the event horizon $z = z_{\text{EH}}(t)$ as follows. For sufficiently late time, spacetimes settle static solutions. Thus, at late time, the event horizon can be easily determined by $F(t, z_{\text{EH}}(t)) = 0$. To determine the event horizon for any t , we solve the null geodesic equations,

$$\dot{z}_{\text{EH}}(t) = -\frac{1}{2}F(t, z_{\text{EH}}(t)) , \quad (5.10)$$

backward along the tangent to the event horizon at late time. Then, we obtain null geodesic generators of the event horizon and find the location of the event horizon $z = z_{\text{EH}}(t)$. Once we know the $z_{\text{EH}}(t)$ and $z_{\text{AH}}(t)$, we can calculate the area of event and apparent horizons as

$$\text{Area}(\text{event/apparent horizon}) = \Phi(t, z_{\text{EH/AH}}(t))^2 . \quad (5.11)$$

In Figure 6, we depict the time evolution of the area of the horizons. We find that the area of the horizons monotonically increase by the time evolution and the event horizon has larger area than that of the apparent horizon. We also see that, after the final state has settled to equilibrium, the apparent horizon and the event horizon coincide. In addition, the two horizons seem to coincide even at the initial state. Thus, it is quite likely that we can regard the area of the horizon as the entropy at the initial state. This issue will be examined further in the following subsection.

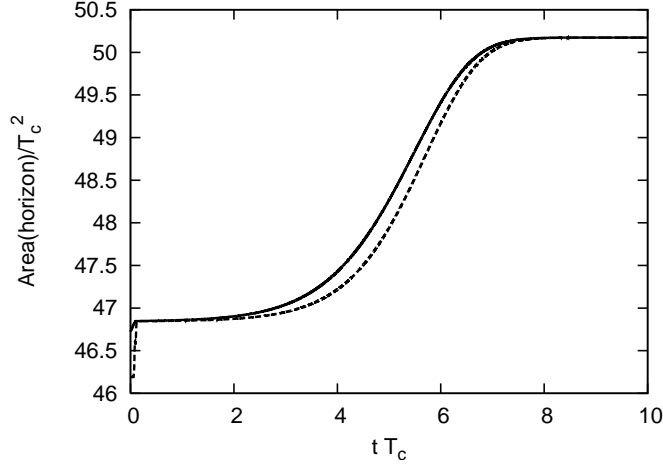


Figure 6: The time evolution of the area of event and apparent horizons are depicted for $q = 1.5$ and $T/T_c = 0.4$ at the initial state. Solid and dashed curves correspond to the area of event and apparent horizons respectively.

5.6 Bulk dynamics and bulk-boundary identification

Having shown properties of the horizons in the bulk, we will discuss how to identify the bulk with the boundary based on observations of the bulk field dynamics. When the system is stationary, we know that the area of the black hole horizon in the bulk corresponds to the entropy of the dual boundary theory. However, there is subtlety in this correspondence for dynamical systems (see, for example, [31–33] and so on). When the system is dynamical, we do not know the mapping between horizons and AdS boundary *a priori*. In other words, there exists ambiguity of the time slices with which we identify the horizon and the boundary. The null time slices we used in this paper, which are illustrated in Figure 1, is nothing but one of the uncountable set of time slices. Thus, we cannot immediately assert that Figure 6 is equivalent to the dynamics of the entropy in the dual theory. In this subsection, we would like to discuss this issue of the identification

Figure 7 shows time dependence of a metric function $\tilde{\Phi}$. In this figure, we show the value of $\dot{\tilde{\Phi}}^2/(zT_c^3)^2$ in gray-scale. The dark region, in which $\dot{\tilde{\Phi}}^2/(zT_c^3)^2$ is large, represents non-stationary region. Rigorously speaking, this figure indicates to what extent a coordinate vector $\xi = \partial/\partial t$ satisfies the Killing equation: $\mathcal{L}_\xi g_{\mu\nu} = \nabla_\mu \xi_\nu + \nabla_\nu \xi_\mu = 0$. The quantity $|\mathcal{L}_\xi g_{\mu\nu}|^2 = 8\dot{\tilde{\Phi}}^2/\Phi^2$ is, however, not always a good indicator of non-equilibrium property since ξ coincides with the timelike Killing vector on the AdS boundary and $|\mathcal{L}_\xi g_{\mu\nu}|^2$ tends

to zero there. In order to examine non-staticity even at the boundary, we focus on the value of $\dot{\tilde{\Phi}}/z$ instead of $\dot{\tilde{\Phi}}$ (see Eq. (3.2)). As we mentioned before, the initial state and the final state are close to equilibrium. It turns out that this fact appears also in Figure 7. Another point we should note is that the shaded region extends almost vertically in this figure. Since we are using null time-slicing, the above fact means that the non-stationary region extends along the ingoing null direction from the boundary to the horizon in the bulk spacetime. Consequently, it may be reasonable to suppose that the mapping between quantities of the boundary and the horizon is given by the null time slices in the current case. It will be interesting to examine whether we can apply this idea to other dynamical systems.

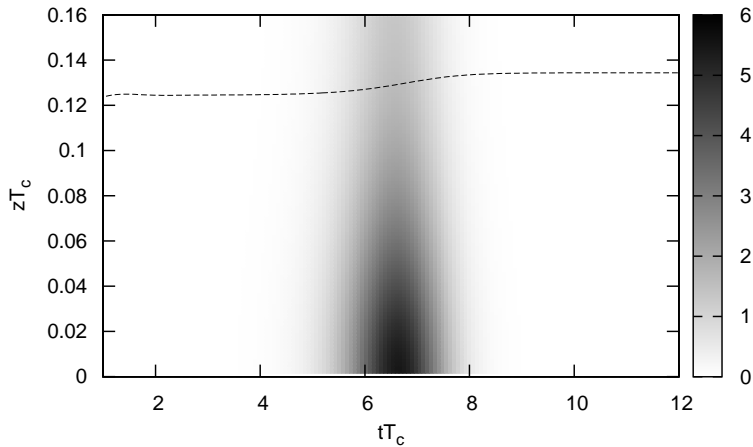


Figure 7: Time dependence of the bulk spacetime for the same parameters used in Figure 6. The value of $\dot{\tilde{\Phi}}^2/(zT_c^3)^2$ is plotted in gray-scale, in which the dark part represents the non-stationary region. In order to examine non-staticity of the entire bulk including the near-boundary region, we have focused on $\dot{\tilde{\Phi}}/z$, which takes finite value even on the AdS boundary, rather than on $\dot{\tilde{\Phi}}$. The dashed curve represents the apparent horizon.

6 Conclusions

We studied the non-equilibrium condensation process in the holographic superconductor by solving the time evolutions of the Einstein-Maxwell-charged scalar system in the asymptotically AdS spacetime. We considered small perturbations on the Reissner-Nordström-AdS black holes, which are static solutions of this system, as the initial states. We found that, when the temperature is lower than the critical temperature T_c , initial perturbations grow exponentially and the spacetimes settle into the hairy black holes obtained in [6]. It is concluded that the hairy black holes are the final states for the instability of the low-temperature Reissner-Nordström-AdS black holes. We also found that the hairy black holes are stable against the plane-symmetric perturbations. As for the superconducting order pa-

parameter in the boundary theory, we clarified how it evolves in non-equilibrium process during the phase transition. As a byproduct, we obtained the relaxation time scale of the order parameter, which is inverse of the imaginary part of the fundamental quasi-normal mode. Finally, we studied the time evolution of the event and apparent horizons and discussed their relevance to the entropy of the boundary theory.

There are many extensions and open issues. One of them is perturbation of dynamical spacetimes obtained in this paper. The dynamics of transport coefficients, such as electrical conductivity or shear viscosity, can be known from the perturbations on the dynamical spacetimes. From the Dirac field perturbation, we may be able to study the Fermi surface properties of superconductors [34–38]. These studies might deepen our understanding on dynamical phenomena in the AdS/CFT correspondence as well as on unknown properties of condensed matter system in non-equilibrium state.

In our calculations, we imposed the plane symmetry, that is, we assumed that the space on (x, y) -plane is homogeneous and isotropic, as in Eq. (2.3). It is interesting to relax this symmetry. For example, we can consider the spacetime with homogeneous and anisotropic (x, y) -plane as

$$ds^2 = -\frac{1}{z^2} (F(t, z)dt^2 + 2dtdz) + \Phi_1(t, z)^2 dx^2 + \Phi_2(t, z)^2 dy^2 . \quad (6.1)$$

The equations of motion for this metric ansatz are given by $(1+1)$ -dimensional PDEs, and thus we can straightforwardly apply the formalism of this paper. In this setting, we can take into account homogeneous electric or magnetic fields along the x or y -directions and study the dynamics of the current in the boundary theory. More challenging problem is to take into account inhomogeneity along one direction, e.g., the y -direction. The equations of motion are given by $(1+2)$ -dimensional PDEs. In the setting, we may holographically realize a system in which the temperature is not homogeneous and the condensed phase and the non-condensed phase coexist. In such an inhomogeneous system, we may observe the thermoelectric phenomena in superconductors [39], such as Peltier effect or the Seebeck effect, or the dynamics of the surface between the two phases [40,41]. Another subject which can be studied by $(1+2)$ -dimensional PDEs is the vortex solution obtained in [42,43]: we must consider the $U(1)$ -symmetric spacetime where the $U(1)$ is the rotational symmetry around the vortex. The spacetime of the vortex solution has a $U(1)$ -symmetry, which is the rotational symmetry around the vortex, and then the equations of motion are again given by $(1+2)$ -dimensional PDEs. Investigation on the non-equilibrium phenomena in these inhomogeneous system and their comparison with theories and experiments in the field of the condensed matter physics may be interesting.

Ultimately, we should study dynamics of spacetimes without any symmetry. Such a task may be tackled only by numerical relativity technique, which is developing rapidly these days [44–48]. To apply this technique to asymptotically AdS spacetime, we have to modify the formalism for asymptotically flat spacetime to accommodate the negative cosmological constant. If such a technique is established, we will be able to investigate on many interesting subjects concerning the non-equilibrium condensation process in the AdS/CFT. For example, it is expected that vortex lattice [49] are formed in a dynamical system from the simulation of the (non-holographic) superconducting system [7–11]. By

simulating its holographic dual in the gravity side using the technique, we will be able to confirm further the AdS/CFT correspondence in a dynamical setup and also may clarify unknown properties of dynamical strongly-coupled systems. We believe that such studies will be fruitful for both of the quantum field theory and general relativity, and our study in this paper will serve as a first step toward such ambitious future issues.

Acknowledgments

We would like to thank Kengo Maeda, Shinji Mukohyama, Harvey S. Reall, Jiro Soda and Takahiro Tanaka for valuable comments on this work. We would also like to thank Paul M. Chesler for kindly teaching us his numerical method in [21]. KM is supported by a grant for research abroad by the JSPS (Japan). SK is the Yukawa Fellow and this work is partially supported by Yukawa Memorial Foundation. This work was supported by the Grant-in-Aid for the Global COE Program "The Next Generation of Physics, Spun from Universality and Emergence" from the Ministry of Education, Culture, Sports, Science and Technology (MEXT) of Japan.

References

- [1] J. M. Maldacena, "The large N limit of superconformal field theories and supergravity," *Adv. Theor. Math. Phys.* **2**, 231 (1998) [*Int. J. Theor. Phys.* **38**, 1113 (1999)] [arXiv:hep-th/9711200].
- [2] S. S. Gubser, I. R. Klebanov and A. M. Polyakov, "Gauge theory correlators from non-critical string theory," *Phys. Lett. B* **428**, 105 (1998) [arXiv:hep-th/9802109].
- [3] E. Witten, "Anti-de Sitter space and holography," *Adv. Theor. Math. Phys.* **2**, 253 (1998) [arXiv:hep-th/9802150].
- [4] S. S. Gubser, "Breaking an Abelian gauge symmetry near a black hole horizon," *Phys. Rev. D* **78**, 065034 (2008) [arXiv:0801.2977 [hep-th]].
- [5] S. A. Hartnoll, C. P. Herzog and G. T. Horowitz, "Building a Holographic Superconductor," *Phys. Rev. Lett.* **101**, 031601 (2008) [arXiv:0803.3295 [hep-th]].
- [6] S. A. Hartnoll, C. P. Herzog and G. T. Horowitz, "Holographic Superconductors," *JHEP* **0812**, 015 (2008) [arXiv:0810.1563 [hep-th]].
- [7] M. Mondello and N. Goldenfeld, "Scaling and vortex dynamics after the quench of a system with a continuous symmetry," *Phys. Rev. A* **42**, 5865 (1990).
- [8] F. Liu, M. Mondello and N. Goldenfeld, "Kinetics Of The Superconducting Transition," *Phys. Rev. Lett.* **66**, 3071 (1991).
- [9] M. Mondello and N. Goldenfeld, "Scaling and vortex-string dynamics in a three-dimensional system with a continuous symmetry," *Phys. Rev. A* **45**, 657 (1992).

- [10] E. Korutcheva and F. Javier de la Rubia, “Dynamical properties of the Landau-Ginzburg Phys. Rev. B **58**, 5153 (1998)
- [11] G. J. Stephens, L. M. A. Bettencourt and W. H. Zurek, “Critical dynamics of gauge systems: Spontaneous vortex formation in 2D superconductors,” Phys. Rev. Lett. **88**, 137004 (2002) [arXiv:cond-mat/0108127].
- [12] R. A. Janik and R. B. Peschanski, “Asymptotic perfect fluid dynamics as a consequence of AdS/CFT,” Phys. Rev. D **73**, 045013 (2006) [arXiv:hep-th/0512162].
- [13] P. Kovtun, D. T. Son and A. O. Starinets, “Viscosity in strongly interacting quantum field theories from black hole physics,” Phys. Rev. Lett. **94**, 111601 (2005) [arXiv:hep-th/0405231].
- [14] S. Bhattacharyya, V. E. Hubeny, S. Minwalla and M. Rangamani, “Nonlinear Fluid Dynamics from Gravity,” JHEP **0802**, 045 (2008) [arXiv:0712.2456 [hep-th]].
- [15] D. Grumiller and P. Romatschke, “On the collision of two shock waves in AdS₅,” JHEP **0808**, 027 (2008) [arXiv:0803.3226 [hep-th]].
- [16] S. S. Gubser, S. S. Pufu and A. Yarom, “Entropy production in collisions of gravitational shock waves and of heavy ions,” Phys. Rev. D **78**, 066014 (2008) [arXiv:0805.1551 [hep-th]].
- [17] L. Alvarez-Gaume, C. Gomez, A. Sabio Vera, A. Tavanfar and M. A. Vazquez-Mozo, “Critical formation of trapped surfaces in the collision of gravitational shock waves,” JHEP **0902**, 009 (2009) [arXiv:0811.3969 [hep-th]].
- [18] S. Lin and E. Shuryak, “Grazing Collisions of Gravitational Shock Waves and Entropy Production in Heavy Ion Collision,” Phys. Rev. D **79**, 124015 (2009) [arXiv:0902.1508 [hep-th]].
- [19] S. S. Gubser, S. S. Pufu and A. Yarom, “Off-center collisions in AdS₅ with applications to multiplicity estimates in heavy-ion collisions,” JHEP **0911**, 050 (2009) [arXiv:0902.4062 [hep-th]].
- [20] S. Bhattacharyya and S. Minwalla, “Weak Field Black Hole Formation in Asymptotically AdS Spacetimes,” JHEP **0909**, 034 (2009) [arXiv:0904.0464 [hep-th]].
- [21] P. M. Chesler and L. G. Yaffe, “Horizon formation and far-from-equilibrium isotropization in supersymmetric Yang-Mills plasma,” Phys. Rev. Lett. **102**, 211601 (2009) [arXiv:0812.2053 [hep-th]].
- [22] I. Amado, M. Kaminski and K. Landsteiner, “Hydrodynamics of Holographic Superconductors,” JHEP **0905**, 021 (2009) [arXiv:0903.2209 [hep-th]].
- [23] S. A. Hartnoll, “Lectures on holographic methods for condensed matter physics,” Class. Quant. Grav. **26**, 224002 (2009) [arXiv:0903.3246 [hep-th]].
- [24] G. T. Horowitz, “Introduction to Holographic Superconductors,” arXiv:1002.1722 [hep-th].

- [25] K. Maeda, M. Natsuume and T. Okamura, “Universality class of holographic superconductors,” *Phys. Rev. D* **79**, 126004 (2009) [arXiv:0904.1914 [hep-th]].
- [26] C. P. Herzog, P. K. Kovtun and D. T. Son, “Holographic model of superfluidity,” *Phys. Rev. D* **79**, 066002 (2009) [arXiv:0809.4870 [hep-th]].
- [27] C. P. Herzog and A. Yarom, “Sound modes in holographic superfluids,” *Phys. Rev. D* **80**, 106002 (2009) [arXiv:0906.4810 [hep-th]].
- [28] K. Maeda, J. i. Koga and S. Fujii, “The final fate of instability of Reissner-Nordström-anti-de Sitter black holes by charged complex scalar fields,” arXiv:1003.2689 [gr-qc].
- [29] R. A. Konoplya, “Decay of charged scalar field around a black hole: Quasinormal modes of R-N, R-N-AdS and dilaton black hole,” *Phys. Rev. D* **66**, 084007 (2002) [arXiv:gr-qc/0207028].
- [30] A. S. Miranda, J. Morgan and V. T. Zanchin, “Quasinormal modes of plane-symmetric black holes according to the AdS/CFT correspondence,” *JHEP* **0811**, 030 (2008) [arXiv:0809.0297 [hep-th]].
- [31] S. Bhattacharyya *et al.*, “Local Fluid Dynamical Entropy from Gravity,” *JHEP* **0806**, 055 (2008) [arXiv:0803.2526 [hep-th]].
- [32] S. Kinoshita, S. Mukohyama, S. Nakamura and K. y. Oda, “A Holographic Dual of Bjorken Flow,” *Prog. Theor. Phys.* **121**, 121 (2009) [arXiv:0807.3797 [hep-th]].
- [33] P. Figueras, V. E. Hubeny, M. Rangamani and S. F. Ross, “Dynamical black holes and expanding plasmas,” *JHEP* **0904**, 137 (2009) [arXiv:0902.4696 [hep-th]].
- [34] C. Wu, K. Sun, E. Fradkin and S. C. Zhang, “Fermi liquid instabilities in the spin channel,” *Phys. Rev. B* **75** (2007) 115103.
- [35] J. W. Chen, Y. J. Kao and W. Y. Wen, “Peak-Dip-Hump from Holographic Superconductivity,” arXiv:0911.2821 [hep-th].
- [36] T. Faulkner, G. T. Horowitz, J. McGreevy, M. M. Roberts and D. Vegh, “Photoemission ‘experiments’ on holographic superconductors,” *JHEP* **1003**, 121 (2010) [arXiv:0911.3402 [hep-th]].
- [37] S. S. Gubser, F. D. Rocha and P. Talavera, “Normalizable fermion modes in a holographic superconductor,” arXiv:0911.3632 [hep-th].
- [38] T. Hartman and S. A. Hartnoll, “Cooper pairing near charged black holes,” arXiv:1003.1918 [hep-th].
- [39] Y. M. Galperin, V. L. Gurevich, V. I. Kozub and A. L. Shelankov, “Theory of thermoelectric phenomena in superconductors,” *Phys. Rev. B* **65**, 064531 (2002)
- [40] O. Ozen and R. Narayanan, “The physics of evaporative and convective instabilities in bilayer systems: Linear theory,” *Physics of Fluids* **16**, 4644 (2004)

- [41] O. Ozen and R. Narayanan “The physics of evaporative instability in bilayer systems: Weak nonlinear theory,” *Physics of Fluids* **16**, 4653 (2004)
- [42] T. Albash and C. V. Johnson, “Vortex and Droplet Engineering in Holographic Superconductors,” *Phys. Rev. D* **80**, 126009 (2009) [arXiv:0906.1795 [hep-th]].
- [43] M. Montull, A. Pomarol and P. J. Silva, “The Holographic Superconductor Vortex,” *Phys. Rev. Lett.* **103**, 091601 (2009) [arXiv:0906.2396 [hep-th]].
- [44] H. Yoshino and M. Shibata, “Higher-dimensional numerical relativity: Formulation and code tests,” *Phys. Rev. D* **80** (2009) 084025 [arXiv:0907.2760 [gr-qc]].
- [45] K. i. Nakao, H. Abe, H. Yoshino and M. Shibata, “Maximal slicing of D-dimensional spherically-symmetric vacuum spacetime,” *Phys. Rev. D* **80** (2009) 084028 [arXiv:0908.0799 [gr-qc]].
- [46] M. Shibata and H. Yoshino, “Nonaxisymmetric instability of rapidly rotating black hole in five dimensions,” *Phys. Rev. D* **81** (2010) 021501 [arXiv:0912.3606 [gr-qc]].
- [47] M. Zilhao, H. Witek, U. Sperhake, V. Cardoso, L. Gualtieri, C. Herdeiro and A. Nerozzi, “Numerical relativity for D dimensional axially symmetric space-times: formalism and code tests,” *Phys. Rev. D* **81**, 084052 (2010) [arXiv:1001.2302 [gr-qc]].
- [48] H. Witek, V. Cardoso, C. Herdeiro, A. Nerozzi, U. Sperhake and M. Zilhao, “Black holes in a box: towards the numerical evolution of black holes in AdS,” arXiv:1004.4633 [hep-th].
- [49] K. Maeda, M. Natsuume and T. Okamura, “Vortex lattice for a holographic superconductor,” *Phys. Rev. D* **81**, 026002 (2010) [arXiv:0910.4475 [hep-th]].